

Brigita Tomšič, Nika Savnik, Elena Shapkova, Laura Cimperman, Lara Šoba, Marija Gorjanc, Barbara Simončič  
University of Ljubljana, Faculty of Natural Sciences and Engineering, Aškerčeva 12, 1000 Ljubljana, Slovenia

# Green In-situ Synthesis of TiO<sub>2</sub> in Combination with *Curcuma longa* for the Tailoring of Multifunctional Cotton Fabric

*Zelena in situ sinteza TiO<sub>2</sub> v prisotnosti ekstrakta kurkume za izdelavo večfunkcionalne bombažne tkanine*

**Original Scientific Paper/Izvirni znanstveni članek**

Received/Prispelo 9-2023 • Accepted/Sprejeto 11-2023

Corresponding author/Korespondenčni avtorica:

**Prof. dr. Barbara Simončič**

E-mail: barbara.simoncic@ntf.uni-lj.si

ORCID: 0000-0002-6071-8829

## Abstract

The introduction of green chemistry has become urgent in the development of innovative, high-performance functional textiles to reduce the environmental footprint of their production. This study aims to develop a new eco-friendly process for the hydrothermal in-situ synthesis of TiO<sub>2</sub> in cotton fabric and dyeing with curcumin natural dye to produce a photocatalytically active coloured textile platform with simultaneous UV protection properties. Two approaches were developed: classical, which included dyeing of the cotton samples with *Curcuma longa* (turmeric) extracts at different concentrations (5 g/L, 10 g/L and 15 g/L) and subsequent hydrothermal in-situ synthesis of TiO<sub>2</sub> in the presence of the dyed cotton samples, and greener, in which simultaneous dyeing with turmeric extracts and hydrothermal in-situ synthesis of TiO<sub>2</sub> were carried out. Since increasing the turmeric concentration hindered the photocatalytic performance of TiO<sub>2</sub> in the chemically modified cotton samples, 5 g/L was selected as the most suitable turmeric concentration. A comparison of the chemical modification processes shows that the simultaneous dyeing of cotton with turmeric extract and hydrothermal in-situ synthesis of TiO<sub>2</sub> was beneficial and resulted in a UV protection factor 50+, which corresponds to excellent protection category. The photocatalytic activity of TiO<sub>2</sub> was maintained in the presence of turmeric, indicating the compatibility of both players in the chemically modified cotton, but not the creation of a turmeric–TiO<sub>2</sub> heterojunction with visible-light-driven photocatalysis. The presence of TiO<sub>2</sub> inhibited the photodegradation of the curcumin dye, further confirming the compatibility of the two players. Keywords: cotton, TiO<sub>2</sub>, turmeric extract, photocatalytic activity, UV protection

## Izveček

Pri razvoju inovativnih, visokozmogljivih funkcionalnih tekstilij je za zmanjšanje okoljskega odtisa pri njihovi proizvodnji postala vpeljava zelene kemije nujna. Zato je bil namen raziskave razviti nov okolju prijazen postopek hidrotermalne in situ sinteze TiO<sub>2</sub> na bombažni tkanini in barvanja z naravnim barvilom kurkume za proizvodnjo fotokatalitsko aktivne obarvane tekstilije s hkratnimi UV-zaščitnimi lastnostmi. Razvita sta bila dva pristopa, in sicer

klasični, ki je vključeval barvanje vzorcev bombaža z izvlečki kurkume različnih koncentracij (5 g/L, 10 g/L in 15 g/L) in naknadno hidrotermalno in situ sintezo  $\text{TiO}_2$  v prisotnosti pobarvanih vzorcev bombaža, in bolj zeleni, kjer sta sočasno potekala barvanje z izvlečki kurkume in hidrotermalna in situ sinteza  $\text{TiO}_2$ . Ker je povečanje koncentracije kurkume oviralo fotokatalitsko delovanje  $\text{TiO}_2$  v kemično modificiranih vzorcih, je bila kot najprimernejša koncentracija kurkume izbrana 5 g/L. Iz primerjave postopkov kemične modifikacije je razvidno, da sta bila sočasno barvanje bombaža z izvlečkom kurkume in hidrotermalna in situ sinteza  $\text{TiO}_2$  zelo učinkovita, s čimer je tkanina dobila UV-zaščitni faktor 50+, kar je kategorizirano kot odlična zaščita. Fotokatalitska aktivnost  $\text{TiO}_2$  se je v prisotnosti kurkume ohranila, kar je kaže na združljivost obeh akterjev v kemično modificiranem bombažu, ni pa se tvoril kompozit kurkuma- $\text{TiO}_2$ , s povečano fotokatalitsko aktivnostjo pri osvetljevanju z vidno svetlobo. Prisotnost  $\text{TiO}_2$  je zavrla fotorazgradnjo kurkume, kar dodatno potrjuje združljivost obeh komponent.

Ključne besede: bombaž,  $\text{TiO}_2$ , ekstrakt kurkume, fotokatalitska aktivnost, UV-zaščita

## 1 Introduction

The chemical modification of textiles is one of the most important textile processes to develop innovative textile materials with desired multifunctional properties. The application of nanomaterials to chemically modify textiles has opened new possibilities for creating new functionalities and improving their properties [1–4]. Among nanomaterials, titanium dioxide ( $\text{TiO}_2$ ) is considered as a versatile inorganic semiconductor material for textile functionalisation with unique electronic structure and functional properties such as photocatalysis, UV protection, antimicrobial activity, thermal stability, biocompatibility, and non-toxicity [5, 6].  $\text{TiO}_2$  is a wide bandgap semiconductor material with photocatalytic self-cleaning properties, i.e., the ability to degrade organic pollutants on its surface under UV light irradiation. Namely, when  $\text{TiO}_2$  is irradiated with UV light in the presence of water and oxygen, it can form reactive oxygen species (ROS) on the surface, which have a strong oxidation potential to degrade organic molecules via intermediates to water and carbon dioxide [7, 8]. The ability to absorb or scatter harmful UV radiation gives  $\text{TiO}_2$  a strong UV-blocking effect, which is crucial for its UV-protection properties.

Growing environmental awareness dictates avoiding the use of conventional chemical modifica-

tion processes as they have a negative impact on the environment due to the consumption of significant amounts of water, energy and chemicals [9, 10]. Therefore, the adoption of eco-friendly approaches is crucial to reducing the environmental footprint. In this context, the application of green chemistry principles, which include the use of safer chemicals, minimising waste and reducing water and energy, plays a crucial role [11]. One of the most important principles of green chemistry is the green synthesis of nanomaterials, which has been extensively studied as an alternative to conventional chemical synthesis processes [12–14]. This also applies to the green synthesis of  $\text{TiO}_2$  [15–22]. It can be carried out in various ways, but plant-mediated biological synthesis, in which plant extracts or phytochemicals can serve as stabilizers, has proven to be one of the most promising and well-implemented. It opens up unlimited resources as different plant parts such as roots, stems, leaves, flowers, fruits and seeds can be used. Since biobased materials are found in nature, they are considered non-toxic and safe, inexpensive, and readily available.

Among plants, *Curcuma longa*, commonly known as turmeric, is a flowering plant of the ginger family. It is known for its rhizomes, which are usually dried and ground into a deep orange-yellow powder called turmeric powder. It is used as a natural yellow dye for textiles and food, as a culinary spice, as a

cosmetic ingredient and as a medicine in traditional herbal medicine [23–25]. According to the literature, turmeric powder has not only established itself for textile dyeing [26–31], but also for the green synthesis of TiO<sub>2</sub> [32–38]. Usually, it is used as an extract prepared in a suitable solvent containing a natural polyphenolic compound called curcumin. When the turmeric extract was combined with the titanium precursor solution under suitable conditions, curcumin acted as a capping agent for the synthesis of TiO<sub>2</sub> and facilitated its formation and stabilisation [39]. Furthermore, when curcumin was in intrinsic contact with TiO<sub>2</sub>, the curcumin molecules could act as a sensitising agent that absorbed visible light, resulting in electron excitation in the curcumin molecule from the highest occupied molecular orbital to the lowest unoccupied molecular orbital, followed by electron transfer from the unoccupied molecular orbital to the conduction band of TiO<sub>2</sub>. This significantly improved the photocatalytic efficiency of TiO<sub>2</sub> upon irradiation with visible light [32–37].

In the present work, a new sustainable approach for the chemical modification of cotton fabric was developed using hydrothermal synthesis of TiO<sub>2</sub> in the presence of curcumin and cotton fabric to create photocatalytic and UV protection properties. Two different application procedures were investigated. The first was a two-step process and involved dyeing of cotton fabric with turmeric extract followed by the in-situ synthesis of TiO<sub>2</sub>. The second was a one-step combination of dyeing with turmeric extract and in-situ synthesis of TiO<sub>2</sub> with the aim of reducing water and energy consumption. In addition, the influence of turmeric extract at different concentrations on the functional properties of TiO<sub>2</sub> was thoroughly investigated. A newly developed innovative chemical modification process for the production of multifunctional textiles represents an important technological shift from conventional to green textile chemistry.

## 2 Experimental

### 2.1 Materials

Alkaline-soured, bleached and mercerized 100% cotton plain-weave fabric (Tekstina d.o.o., Ajdovščina, Slovenia), with a mass per unit area of 120 g/m<sup>2</sup>, was used for chemical modification. Turmeric powder (Maestro, Podravka d.d., Croatia) was bought at a local market. Titanium(IV) isopropoxide (TTIP; ≥ 97.8% concentration), isopropanol (≥ 99% concentration) and acetic acid were procured from Sigma Aldrich (United States), Honeywell Research Chemicals (Seetze, Germany) and CARLO ERBA Reagents S.A.S (Barcelona, Spain), respectively.

### 2.2 Preparation of the turmeric extract

The extract of turmeric powder was prepared in distilled water at three different concentrations: 5 g/L, 10 g/L and 15 g/L. A certain amount of the powder was covered with cold distilled water, heated and boiled for 5 minutes. Then, the boiled solution was cooled and filtered. For each concentration, 2 L of extract was prepared. The *Curcuma longa* rhizomes, their powder, the cooled extract solution (5 g/L) and the chemical structure of the natural dye curcumin are shown in Figure 1.

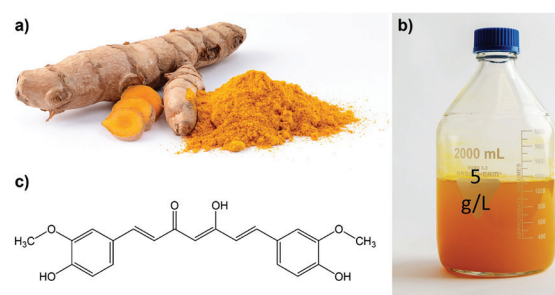


Figure 1: *Curcuma longa* rhizomes and their powder (a), the turmeric extract (b), and the chemical structure of the enol form of the curcumin natural dye in the turmeric extract (c).

### 2.3 Chemical modification of cotton fabric

Chemical modification of cotton fabric was carried out in two different processes. The first classical process involved two steps: the dyeing of cotton samples with turmeric extract followed by the in-situ synthesis of  $\text{TiO}_2$  on the dyed samples. For this purpose, 7 g cotton samples were dyed with 5 g/L, 10 g/L and 15 g/L turmeric extracts (three samples for each extract concentration) by exhaustion with a 1:20 ratio of good to liquor for 40 minutes at 40 °C in the Starlet laboratory dyeing machine (Daelim Starlet, Co., Korea). After dyeing, the samples were squeezed on a two-roll padder (Mathis, Switzerland) with a wet pickup of  $100\% \pm 5\%$  and air-dried. For the in-situ synthesis of  $\text{TiO}_2$ , the TTIP sol (200 g) was previously prepared as a 4% hydrolysed dilution of the TTIP precursor (8 g) in isopropanol (182 g) by adding acetic acid (10 g) and stirred magnetically for about two hours until hydrolysis was completed. The dyed samples were immersed in the TTIP sol and then squeezed out on a two-roll padder with a wet pickup of  $100\% \pm 5\%$  and dried at 100 °C for 1 minute in the laboratory drying apparatus (Mathis, Switzerland). Subsequently, each sample was immersed in 350 g of water and hydrothermally treated for 90 min at 120 °C in the Starlet laboratory dyeing machine. Finally, the samples were squeezed with a wet pickup of  $100\% \pm 5\%$  and air-dried.

The second greener process involved the simultaneous dyeing of cotton samples with turmeric extracts and the in-situ synthesis of  $\text{TiO}_2$ . For this purpose, a hydrolysed TTIP sol was applied to the undyed cotton samples in the same way as in the first procedure (immersion in the TTIP sol, squeezing with a wet pickup of  $100\% \pm 5\%$  and drying for 1 min at 100 °C), followed by the immersion of the samples in 350 g turmeric solutions of different concentrations (three samples for each extract concentration) and hydrothermal treatment for 90 min at 120 °C, squeezing, and drying. For comparison, the dyeing of cotton samples in 5 g/L turmeric extract solution and the in-situ synthesis of  $\text{TiO}_2$  were also performed under the same conditions as the two

processes. The sample codes for the chemical modification processes are summarized in Table 1.

Table 1: Sample codes according to the chemical modification process

Sample code	Chemical modification process
UN	Untreated (no chemical modification)
C5	Dyeing of the cotton sample with 5 g/L turmeric extract
T	Hydrothermal in-situ synthesis of $\text{TiO}_2$ from 4% TTIP in the presence of an undyed cotton sample
C5-T	Dyeing of the cotton sample with 5 g/L turmeric extract followed by the hydrothermal in-situ synthesis of $\text{TiO}_2$ from 4% TTIP in the presence of the dyed cotton sample
C10-T	Dyeing of the cotton sample with 10 g/L turmeric extract followed by the hydrothermal in-situ synthesis of $\text{TiO}_2$ from 4% TTIP in the presence of the dyed cotton sample
C15-T	Dyeing of the cotton sample with 15 g/L turmeric extract followed by the hydrothermal in-situ synthesis of $\text{TiO}_2$ from 4% TTIP in the presence of the dyed cotton sample
C5+T	Simultaneous dyeing of the cotton sample with 5 g/L turmeric extract and hydrothermal in-situ synthesis of $\text{TiO}_2$ from 4% TTIP
C10+T	Simultaneous dyeing of the cotton sample with 10 g/L turmeric extract and hydrothermal in-situ synthesis of $\text{TiO}_2$ from 4% TTIP
C15+T	Simultaneous dyeing of the cotton sample with 15 g/L turmeric extract and hydrothermal in-situ synthesis of $\text{TiO}_2$ from 4% TTIP

### 2.4 Analysis and measurements

#### 2.4.1 Scanning electron microscopy (SEM) and energy-dispersive X-ray spectroscopy (EDS)

The morphological characteristics of samples UN, C5, T, C5-T and C5+T were determined using the scanning electron microscope JSM-6060 LV (JEOL, Japan). Each sample was imaged three times at a different location at 3000- $\times$  magnification. Before imaging, the samples were coated with a thin layer of gold to ensure conductivity.

In addition, the samples were examined using the Thermo Fischer Scientific Quattro S energy dispersive field emission scanning electron microscope (Thermo Fisher Scientific, USA), which works at an accelerating voltage of 1 kV in high vacuum and uses a concentric backscattered electron detector (CBS). An energy dispersive detector (Oxford Instruments Ultim Max 65) was used to verify the chemical composition of the observed particles using AZtec software. EDS spectra and elemental mappings of C, Ti and O were obtained. The samples were coated with a thin carbon layer before analysis.

#### 2.4.2 Add-on

The total quantity of dry solid add-on of the samples UN, C5, T, C5-T and C5+T was determined using an electronic moisture analyser (KERN MLB-C). The samples were preconditioned for 24 h at 65% relative humidity and 20 °C. They were then dried at 105 °C until a constant mass was reached, i.e. until the change in weight within 120 s was less than 1 mg. The add-on value was calculated according to the following equation:

$$\text{Add-on} = \frac{(m_2 - m_1)}{m_1} \cdot 100 (\%) \quad (1)$$

where  $m_2$  is the mass of the finished sample and  $m_1$  is the mass of the untreated sample.

#### 2.4.3 Inductively coupled plasma-mass spectrometry (ICP-MS)

The concentrations of Ti in the samples T, C5-T and C5+T were determined via ICP-MS using a Perkin Elmer SCIED Elan DRC spectrophotometer. A 0.5 g sample was prepared in a Milestone microwave system via acid decomposition with 65% HNO<sub>3</sub> and 30% H<sub>2</sub>O<sub>2</sub>. Ti concentrations were reported as the mean values of two measurements for each sample. Based on the measured Ti values, the TiO<sub>2</sub> concentration was calculated.

#### 2.4.4 X-ray diffraction analysis (XRD)

X-ray diffraction (XRD) patterns of the crystal phase of samples UN, T, C5-T and C5+T were recorded using a Philips PW3830 X-ray diffractometer equipped with Cu-Kα1 1.54060 Å radiation and a secondary graphite monochromator. Data were recorded at 40 kV and a current of 30 mA over a range of 10° to 90° 2θ at a rate of 3° per minute. Diffraction patterns were obtained using X'Pert HighScore Plus software ver. 4.8.

#### 2.4.5 Fourier transform infrared spectroscopy (FTIR)

The chemical composition of the samples UN, C5, T, C5-T and C5+T was analysed using FTIR spectrometer Spectrum 3 (Perkin Elmer, UK). Spectra between 4000 cm<sup>-1</sup> and 600 cm<sup>-1</sup> were recorded with a resolution of 4 cm<sup>-1</sup> and an average of 120 spectra per sample.

#### 2.4.6 Colour measurements

Colour measurements of the samples UN, C5-T, C10-T, C15-T, C5+T, C10+T and C15+T were performed using a Spectrophotometer Spectraflash 600 PLUS CT (Datacolor, Switzerland). The reflectance,  $R$ , of each sample was measured five times at different locations, and the average value was calculated. The colour strength,  $K/S$  value, was calculated from the following equation [40]:

$$\frac{K}{S} = \frac{(1-R)^2}{2R} \quad (2)$$

where  $R$  is the reflectance of the dyed samples at  $\lambda_{max}$ ,  $K$  is the absorption coefficient and  $S$  is the scattering coefficient of the sample.

#### 2.4.7 UV-Vis spectroscopy and determination of the UV protection properties

The transmission and reflection spectra of the samples UN, C5-T, C10-T, C15-T, C5+T, C10+T and C15+T were recorded in the wavelength range 250–750 nm using a Lambda 850+ UV/Vis spectrophotometer

(Perkin Elmer, United Kingdom) equipped with a reflection module—a 150 mm integration sphere—and fully controlled by a computer running WinLab 6 UV software. Three measurements were made for each sample at different angles of warp alignment, and the average value of transmittance,  $T$ , and reflectance,  $R$ , at each wavelength was calculated. Using the UV transmission spectra, the UV protection properties of the samples were determined according to the standard EN 13758-1: 2001. The main values of  $T$  were calculated at wavelengths of 315–400 nm (UVA), 290–315 nm (UVB) and 290–400 nm (UVR). The ultraviolet protection factor, UPF, was calculated as follows [41]:

$$\text{UPF} = \frac{\sum_{290}^{400} E(\lambda) \cdot \varepsilon(\lambda) \cdot \Delta\lambda}{\sum_{290}^{400} E(\lambda) \cdot \varepsilon(\lambda) \cdot T(\lambda) \cdot \Delta\lambda} \quad (3)$$

where  $E(\lambda)$  is the solar spectral irradiance,  $\varepsilon(\lambda)$  is the relative erythral effectiveness,  $\Delta(\lambda)$  is the wavelength interval and  $T(\lambda)$  is the spectral transmittance at the wavelength  $\lambda$ .

UPF rating and protection categories were determined using UPF values, calculated according to the Australian/New Zealand Standard for Sun-Protective Clothing—Evaluation and Classification (AS/NZS 4399, 2020), where UPF values of 15– correspond to the “minimum protection” category, UPF values of 30– correspond to the “good protection” category and UPF values of 50– correspond to the “excellent protection” category.

#### 2.4.8 Photocatalytic activity

The photocatalytic activity of chemically modified cotton samples was investigated using the photocatalytic degradation of Rhodamine B (RhB) dye solution under UV and visible light illumination. For this purpose, the samples UN, C5-T, C10-T, C15-T, C5+T, C10+T and C15+T with a size of 1 cm × 3 cm were immersed in 5 ml of 0.025 mM RhB solution in a Petri dish and exposed to UV light for 60, 120, 180 and 240 minutes in the Color Control Professional chamber (Just Normlicht – Vertriebs GmbH, Germany).

In addition, the samples UN, C5, T, C5-T and C5+T were also placed in a cuvette filled with 3 ml of 0.025 mM RhB solution and illuminated in a Xenotest Alpha instrument (Atlas, USA), equipped with a visible xenon arc lamp (radiation attitude 0.8–2.5 kVA and extended radiation range 300–400 nm). The cuvettes were illuminated for 30, 60, 120, 160 and 240 minutes. After each illumination time, the absorbance of the RhB solution was measured at  $\lambda_{max}$  and the corresponding concentration of RhB dye was determined using a previously prepared calibration curve. Measurements were performed using a Lambda 850+ UV/Vis spectrophotometer (Perkin Elmer, United Kingdom). The RhB dye degradation efficiency was calculated as the percentage of dye degradation,  $D$ , as follows [42]:

$$D = \frac{(c_0 - c_t)}{c_0} \cdot 100 (\%) \quad (4)$$

where  $c_0$  is the concentration of the RhB dye solution before illumination and  $c_t$  is the concentration of the RhB dye solution after a certain time of illumination. For comparison, the photodegradation of the 0.01 mM Methylene blue (MB) dye solution in the presence of the T, C5-T and C5+T samples was also carried out in a Xenotest Alpha instrument under the same conditions as in the case of the RhB dye solution.

#### 2.4.9 Colour fastness to light

The colour fastness of samples C5, C5-T and C5+T to xenon light was tested in accordance with the standard SIST EN ISO 105-B02:2014. The samples were exposed to light in a Xenotest alpha apparatus (Atlas, USA) for a specified time (72 hours). Light fastness was assessed by the colour difference,  $\Delta E_{ab}^*$ . For this purpose, ten measurements of the colour coordinates  $L^*$ ,  $a^*$  and  $b^*$  in the CIELAB colour space were made for each sample examined using a Datacolor Spectro 1050 spectrophotometer (Datacolor, USA). The measurements were performed with a 9 mm aperture under D65 illumination and an observation

angle of 10°. The value of  $\Delta E_{ab}^*$  was calculated using the following equation [40]:

$$\Delta E_{ab}^* = \sqrt{(\Delta L^*)^2 + (\Delta a^*)^2 + (\Delta b^*)^2} \quad (5)$$

where  $\Delta L^*$ ,  $\Delta a^*$  and  $\Delta b^*$  are the differences in the lightness, green–red, and blue–yellow colour coordinates, respectively, calculated between the illuminated and non-illuminated samples.

### 3 Results and discussion

The influence of the concentration of turmeric extract and the process of chemical modification on the colour yield of the cotton samples is shown in Figure 2. From both the photographs (Figure 2a) and the  $K/S$  values (Figure 2b), it can be seen that increasing the concentration of turmeric extract from 5 g/L to 10 g/L significantly increased the colour yield of the samples in both modification processes.

Accordingly, the  $K/S$  values increased from 0.4 for sample C5-T to 0.68 for sample C10-T and from 0.73 for sample C5+T to 1.71 for sample C10+T. In contrast, the additional increase in concentration from 10 g/L to 15 g/L turmeric extract did not contribute to colouration of the samples and even resulted in a slight decrease in colour yield. It is also clearly seen that at the same concentration of turmeric extract, the  $K/S$  values of samples C5+T, C10+T and C15+T are significantly higher compared to samples C5-T, C10-T and C15-T. This indicates that the chemical modification process strongly influenced the intensity of the colouration of the samples. Definitely, the colour strength of curcumin dye was higher in the chemical modification process involving the simultaneous dyeing of the cotton samples with turmeric extract and hydrothermal in-situ synthesis of TiO<sub>2</sub> than in the process where the samples were previously dyed with the turmeric extract followed by the hydrothermal in-situ synthesis of TiO<sub>2</sub> in the presence of the dyed cotton samples.

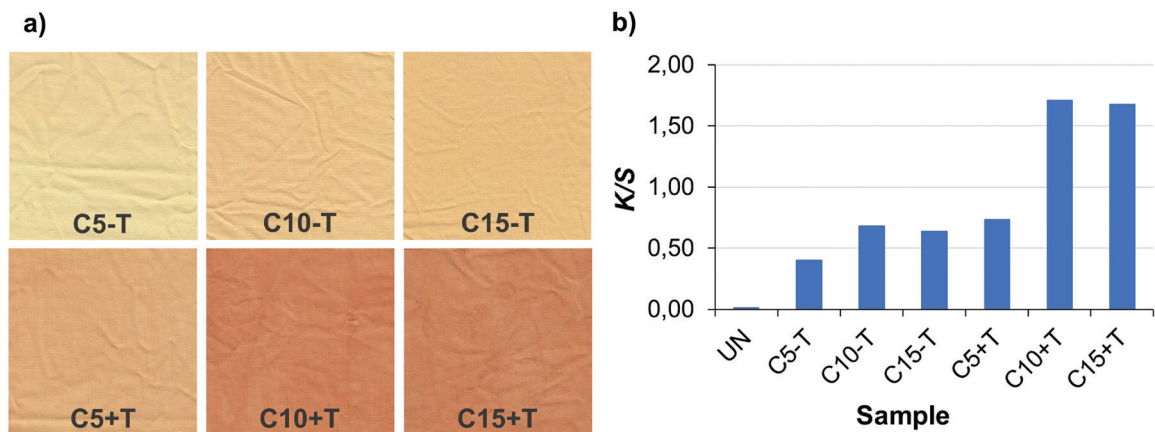


Figure 2: Photos of the chemically modified cotton samples (a);  $K/S$  values of untreated and chemically modified cotton samples (b)

To gain insight into the influence of the curcumin dye and TiO<sub>2</sub> on the functional properties of the chemically modified cotton samples, the UPF values and the efficiency of degradation of the RhB dye were determined (Figure 3). The results in Figure 3a show that the chemical modification of the cotton samples

resulted in a dramatic improvement in UV protection properties, as reflected by an increase in UPF values from 4.1 for sample UN to 42.2, 47.5 and 40.1 for samples C5-T, C10-T and C15-T, respectively, and to 53.2, 58.0 and 77.9 for samples C5+T, C10+T and C15+T. The UPF values of all three samples

C5-T, C10-T and C15-T correspond to the “good protection” category, and the UPF values of all three samples C5+T, C10+T and C15+T correspond to the “excellent protection” category. These results clearly show that simultaneous dyeing with turmeric extract and hydrothermal in-situ synthesis of  $\text{TiO}_2$  is beneficial to achieving maximum protection of cotton fabric against UV radiation. The highest UPF value was obtained for sample C15+T, in which the highest concentration of turmeric extract was used.

The efficiency of the chemically modified cotton samples for the degradation of the RhB dye solution was investigated under UV illumination, which is crucial for the photocatalytic activity of  $\text{TiO}_2$ . The results in Figure 2b clearly show that the photocatalytic degradation of the RhB dye solution was more efficient in the presence of samples C5-T, C10-T and C15-T than in the presence of samples C5+T, C10+T and C15+T, which is contrary to the results obtained for the UV protection properties. In terms of photocatalytic performance, it is reasonable to conclude that the chemically modified cotton samples prepared via the process in which  $\text{TiO}_2$  synthesis was carried out in the presence of the previously dyed

samples provided a more efficient photocatalytic platform for RhB dye degradation than the cotton samples prepared via simultaneous dyeing and  $\text{TiO}_2$  synthesis. Moreover, increasing the concentration of curcumin dye on the cotton samples hindered the photocatalytic efficiency of  $\text{TiO}_2$ , as the cotton samples dyed with 5 g/L turmeric extract exhibited the highest percentage of photodegraded RhB dye at all degradation time intervals. This phenomenon is particularly evident in the C5+T, C10+T and C15+T samples, where the  $\text{TiO}_2$  was synthesised in the turmeric extract. This suggests that the curcumin dye forms the composites with  $\text{TiO}_2$  in which it covers the  $\text{TiO}_2$  particles and hinders the  $\text{TiO}_2$  photocatalytic activity at higher dye concentrations. After considering both results, i.e., UPF and photocatalytic efficiency, samples C5-T and C5+T were selected as representative samples with the optimal multifunctional properties tailored with the combination of curcumin dye and  $\text{TiO}_2$  in both chemical modification processes and were therefore used for further investigations in comparison to the chemically modified samples with solei  $\text{TiO}_2$  or curcumin dye.

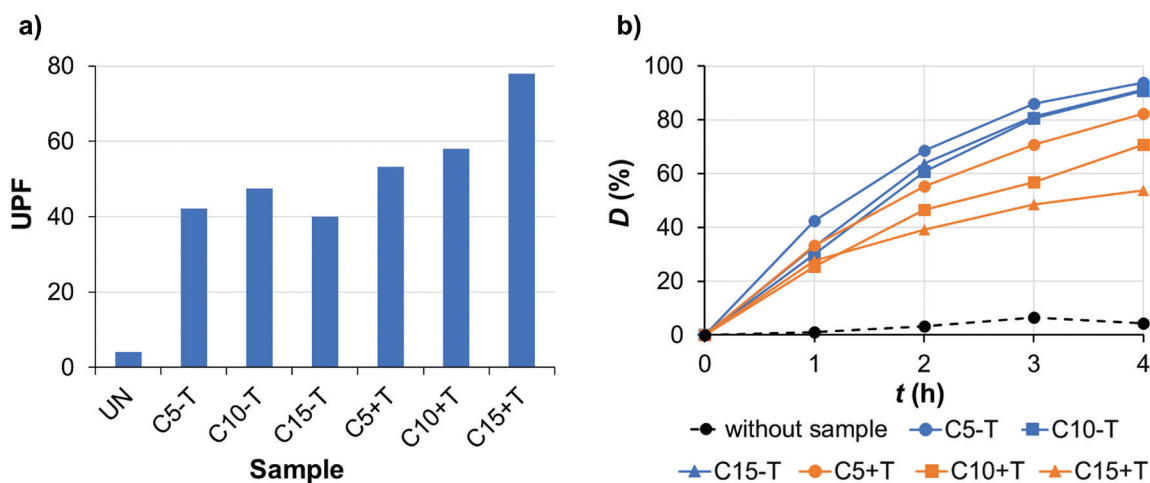


Figure 3: UPF of untreated and chemically modified cotton samples (a), photocatalytic degradation of the RhB dye solution without and in the presence of chemically modified cotton samples after different illumination times under UV light (b)

The SEM images of samples UN, C5, T, C5-T and C5+T are shown in Figure 4. As can be seen in the SEM image of sample UN, the untreated cellulose

fibres have a typical ribbon-like structure with a smooth and even surface, showing some natural impurities. Dyeing of the cotton samples with turmeric

extract did not cause any visible morphological surface changes in the cellulose fibres (sample C5). In contrast, in-situ synthesis of  $\text{TiO}_2$  particles resulted in an increase in the roughness of the cellulose fibres with a clearly visible thin  $\text{TiO}_2$  coating containing many small and larger  $\text{TiO}_2$  agglomerates (samples T, C5-T and C5+T). This phenomenon is most pronounced in sample C5+T.

The successful in-situ synthesis of  $\text{TiO}_2$  on the

cellulose fibres was confirmed by the EDS analysis, which is shown in Figure 5 for the representative sample T. From the EDS spectrum in Figure 5b, obtained from the part of Figure 5a marked with a yellow frame, and from the element mapping images in Figure 5c, it is clear that sample T contains Ti, O and C elements in the structure. The EDS analysis also confirms that the white spots in Figure 5a represent  $\text{TiO}_2$  particles.

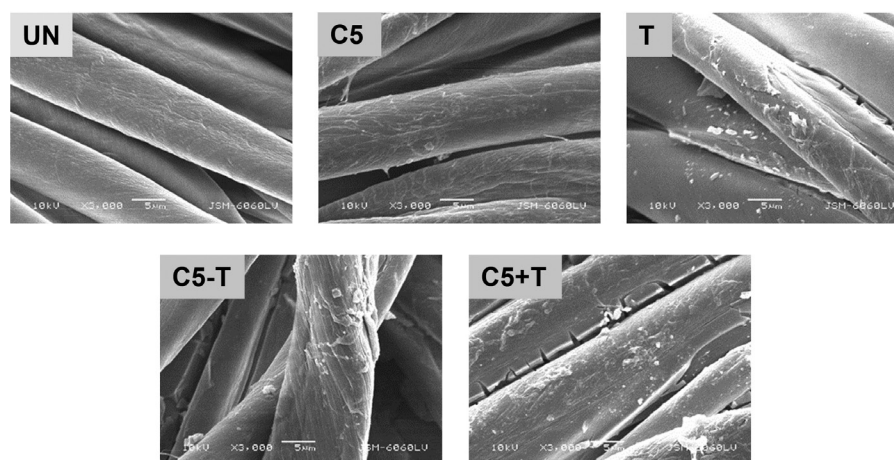


Figure 4: SEM images of the untreated and chemically modified cotton samples at 3000x magnification

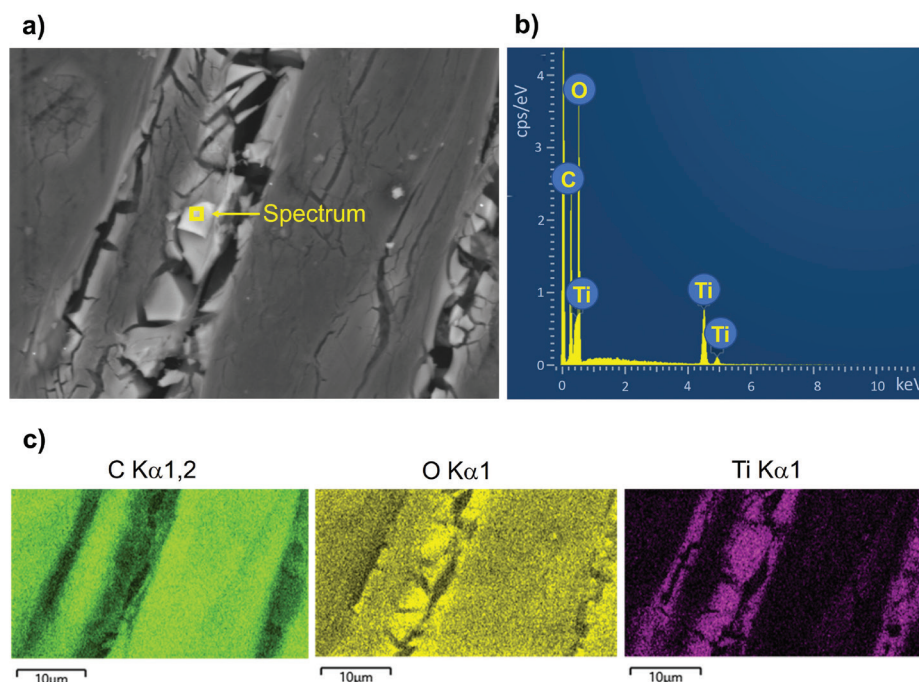


Figure 5: SEM/BSE image of the sample T with the position of the EDS analysis (a), EDS spectrum (b) and element mapping images of C, O, and Ti (c) in the sample T

The total content of  $\text{TiO}_2$  in samples T, C5-T and C5+T was determined by calculating the dry solid add-on and using ICP-MS analysis (Table 2). From Table 2, the amount of  $\text{TiO}_2$  synthesised with the same 4% TTIP sol was highest in sample C5+T, followed by sample T, and the lowest amount was obtained in sample C5-T. This indicates that the hydrothermal in-situ synthesis of  $\text{TiO}_2$  was promoted in turmeric extract (sample C5+T) compared to water (sample T). In contrast, the presence of curcumin dye in the previously dyed cotton samples slightly decreased the amount of  $\text{TiO}_2$  synthesised (sample C5-T). Based on these results, the simultaneous dyeing of cotton samples with turmeric extract and hydrothermal in-situ synthesis of  $\text{TiO}_2$  is favourable for the production of chemically modified cotton fabric.

Table 2: Dry solid add-on and the concentration of  $\text{TiO}_2$  in the chemically modified samples included  $\text{TiO}_2$

Sample	m (g)	Add-on (%)	c $\text{TiO}_2$ (mg/kg)
UN	0.287	/	/
T	0.291	1.39	8600
C5-T	0.289	0.70	8000
C5+T	0.295	2.79	8900

The XRD analysis of the samples UN, T, C5-T and C5+T shown in Figure 6 provided valuable information about the crystal phases of the in-situ synthesised  $\text{TiO}_2$  in the cotton samples. The XRD pattern of sample UN shows well-defined diffraction peaks at  $2\theta = 15.0^\circ$ ,  $16.8^\circ$ ,  $22.7^\circ$  and  $34.5^\circ$ , corresponding to the (110),  $(11\bar{0})$ , (200) and (400) crystallographic planes of the crystalline structure of cellulose, respectively [43]. As expected, these peaks are also clearly visible in samples T, C5-T and C5+T. The prominent diffraction peaks at  $2\theta = 25.3^\circ$ ,  $37.8^\circ$  and  $48^\circ$ , corresponding to the (101), (220) and (022) crystallographic planes of the anatase crystalline phase of  $\text{TiO}_2$  [44], could not be detected in samples T, C5-T and C5+T, suggesting that the in-situ synthesised  $\text{TiO}_2$  has an amorphous structure. This is plausible, since the hydrothermal in-situ synthesis of  $\text{TiO}_2$  was carried out at  $120^\circ\text{C}$ , which is too low for

the calcination of  $\text{TiO}_2$  to produce crystalline phases. The same results have been reported in the literature [44–46].

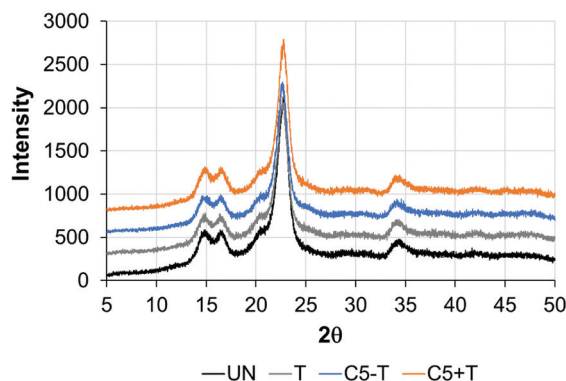


Figure 6: XRD patterns of the samples UN, T, C5-T and C+T

The influence of curcumin dye and  $\text{TiO}_2$  on the chemical properties of the chemically modified cotton samples was determined by FTIR analysis (Figure 7). The IR ATR spectrum of the sample UN showed the absorption bands characteristic of the cellulose fingerprint in the  $1500\text{--}800\text{ cm}^{-1}$  region, corresponding to C–H, C–O, C–C C–O–C and O–H vibrations [47]. A comparison of the IR ATR spectrum of sample C5 with that of sample UN revealed no significant changes. This suggests that the characteristic bands of turmeric occurring at  $1740\text{--}1680\text{ cm}^{-1}$  due to C=O absorption, at  $\sim 1510\text{ cm}^{-1}$  due to aromatic skeletal stretching vibration and at  $\sim 1030\text{ cm}^{-1}$  due to C–OH stretching vibration were blurred by the strong vibrational bands of cellulose [48]. In addition, the characteristic bands of  $\text{TiO}_2$  in samples T, C5-T and C5+T, which appear at  $700\text{--}600\text{ cm}^{-1}$ , could not be detected by FTIR analysis due to the low concentration of  $\text{TiO}_2$  [47]. The  $\text{TiO}_2$  vibrations that appear at wavenumbers below  $600\text{ cm}^{-1}$  could not be analysed.

Transmission and reflection spectra were recorded to determine the influence of the curcumin dye and  $\text{TiO}_2$  on the UV protection properties of the chemically modified cotton samples (Figure 8, Table 3). From Figure 8a, it can be seen that the transmission

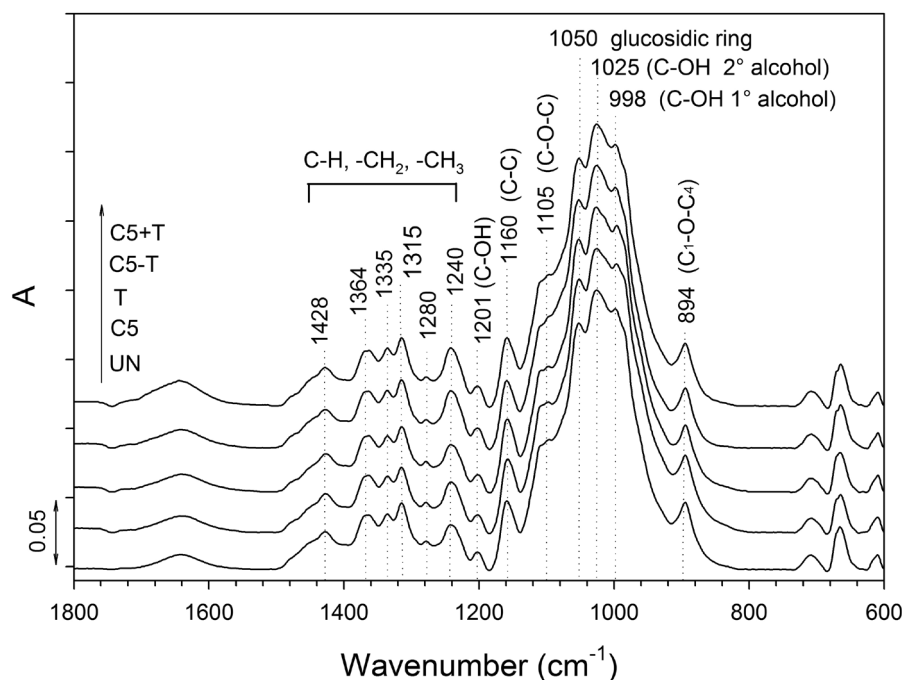


Figure 7: IR ATR spectra of the samples UN, C5, T, C5-T and C+T

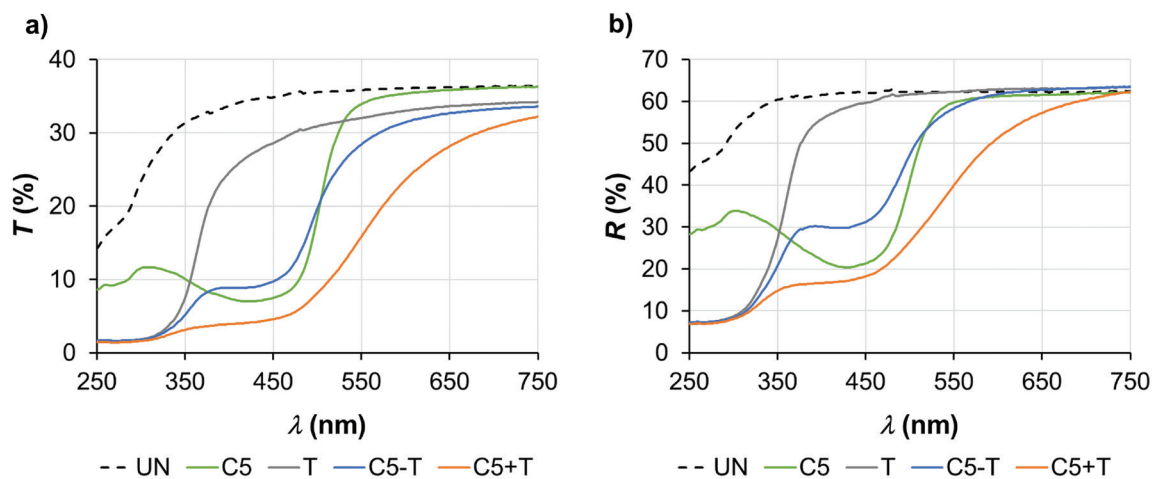


Figure 8: Transmission (a) and reflection (b) spectra of the samples UN, C5, T, C5-T and C5+T.

of UV rays (250–400 nm) through the sample UN was between 15% and 35%, which was too high to provide UV protection properties. Accordingly, the UPF of the sample UN was very low (3.86 in Table 3). The presence of curcumin dye reduced the transmission of UV rays through sample C5 compared to sample UN with  $T$  values of 9.52% for the UVA region and 11.41% for the UVB region (Table 3). However, the  $T$  values of about 10% were too high to provide minimal

UV protection. In contrast to the curcumin dye, the presence of TiO<sub>2</sub> drastically reduced the transmission of UV rays in the UVB (290–315 nm) region, but in the UVA (315–400 nm) region, the transmission increased significantly and even exceeded that of sample C5 (Figure 8a). This resulted in a UPF value of 34.29, which is categorized as good protection. The combination of the curcumin dye with TiO<sub>2</sub> in samples C5-T and C5+T improved their UV

protection properties. In particular, at UVA, the synergism between the curcumin dye and  $\text{TiO}_2$  led to a significant reduction in  $T$  values to 6.04 and 3.15 for samples C5-T and C5+T, respectively. This resulted in a UPF value of 42.17 for sample C5-T and 53.24 for sample C5+T. The latter is in the 50+ category, which corresponds to excellent protection. Since the

reflection spectra of samples C5, T, C5-T and C5+T (Figure 8b) are lower than the spectrum of sample UN, this suggests that the UV blocking mechanism of  $\text{TiO}_2$  is based on the absorption of UV light. As expected, the same phenomenon was observed for the curcumin dye due to the absorption capacity of the conjugated system in its aromatic structure.

Table 3: The arithmetic mean of transmittance,  $T$ , in the UVA, UVB and UVR ranges and the UVR protection categories for the untreated and functionalised cotton samples according to the Australian/New Zealand Standard Sun-Protective Clothing—Evaluation and Classification

Sample	$T$ (UVA) (%)	$T$ (UVB) (%)	$T$ (UVR) (%)	UPF	UVR protection category <sup>a)</sup>
UN	31.28	23.71	29.53	3.86	NR
C5	9.52	11.41	9.96	8.75	NR
T	12.43	1.91	9.98	34.29	G
C5-T	6.04	1.87	5.07	42.17	G
C5+T	3.15	1.64	2.80	53.24	E

<sup>a)</sup> NR – non rateable, G – good protection, E – excellent protection

The photocatalytic activity of  $\text{TiO}_2$  in the cotton samples without and with the presence of the curcumin dye was investigated using the rate of degradation of RhB and MB dyes under visible light illumination (Figure 9). Visible light illumination was chosen to determine whether the presence of the curcumin dye in samples C5-T and C5+T could act as a sensitizer and have a photosensitisation effect on the visible-light-induced photocatalytic performance of  $\text{TiO}_2$ . The results in Figure 9a clearly show that, as expected, samples UN and C5 did not exhibit photocatalytic activity, resulting in insignificant photodegradation of the RhB dye solution, which was still coloured after 4 hours of illumination, very similar to the blank solution without a sample (Figure 9c). In contrast, the photodegradation of the RhB dye solution in the presence of samples T, C5-T and C5+T was very efficient, with the percentage of dye degradation being over 95% in 2 hours of illumination and almost 100% in 4 hours of illumination, resulting in the complete decolourisation of the RhB dye solution (Figure 9c). A close inspection of Figure 9a reveals that the presence of the curcumin dye slightly hindered the photodegradation performance of

$\text{TiO}_2$  at the beginning of the illumination compared to sample T. However, the photodegradation performance of samples C5-T and C5+T was comparable to that of sample T at longer illumination times. In the experiment on the photodegradation of the MB dye (Figure 9b), the C5+T sample showed slightly higher photocatalytic activity than the T and C5-T samples after 1 hour of illumination; however, this phenomenon did not occur at longer illumination times, when the photodegradation efficiency of the T, C5-T and C5+T samples was very similar (Figure 9b). Comparison of the results in Figure 9a and Figure 9b also shows that the photodegradation efficiency of the T, C5-T and C5+T samples is slightly higher for the RhB dye than for the MB dye, resulting in a photodegradation of more than 98% for the RhB dye and about 95% for the MB dye after 4 hours of illumination. This indicates that the chemical structure of the dye influences the photodegradation efficiency of the photocatalyst, which is consistent with literature data [49].

The results in Figure 9 clearly indicate that the photocatalytic activity of  $\text{TiO}_2$  was maintained in the presence of the curcumin dye but was not en-

hanced under visible light. The curcumin dye definitely did not act as a sensitizer for TiO<sub>2</sub> in samples C5-T and C5+T. It can be concluded that the two chemical modification processes investigated do

not provide the conditions for the creation of a curcumin-TiO<sub>2</sub> heterojunction with visible-light-driven photocatalysis.

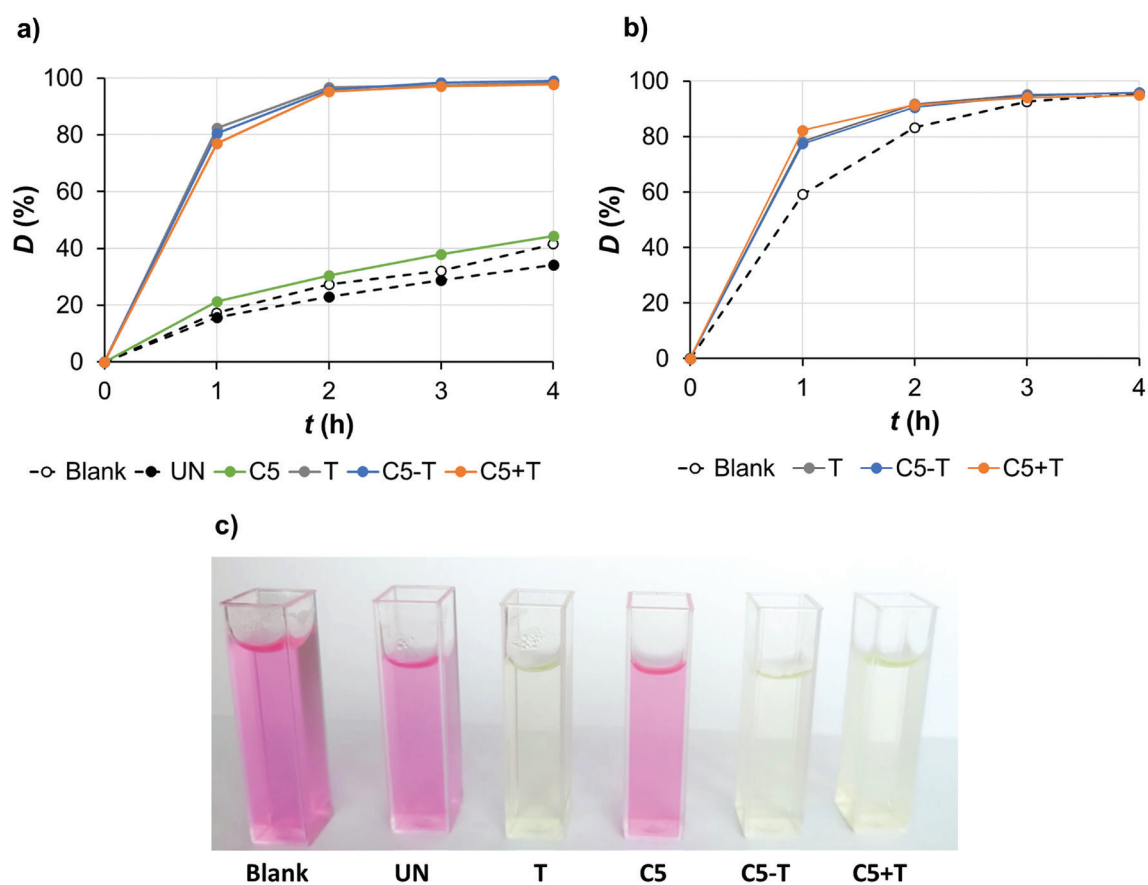


Figure 9: Photocatalytic degradation of RhB (a) and MB (b) dyes solution without sample (blank) and in the presence of samples UN, C5, T, C5-T, and C5+T after different illumination times under visible light; photos of RhB dye solution after 4 hours of radiation without and in the presence of the samples (c)

To verify whether the photocatalytic effect of TiO<sub>2</sub> causes photodegradation of the curcumin dye in samples C5-T and C5+T, the colour fastness of these samples was determined in comparison to sample C5 without TiO<sub>2</sub> and the results are shown in Table 4. It can be seen that the colour of all samples faded during illumination, resulting in high values of  $\Delta E_{ab}^*$ . This phenomenon was expected as it is known that most natural dyes have poor colour fastness to light, which is also true for curcumin [50]. However, the results in Table 4 show that the

highest value of  $\Delta E_{ab}^*$  was obtained for sample C5 and that this value was much higher than the  $\Delta E_{ab}^*$  values of samples C5-T and C5+T, indicating that the presence of TiO<sub>2</sub> did not promote but rather inhibited the photodegradation of the curcumin dye, confirming the compatibility of the curcumin and TiO<sub>2</sub> in the chemically modified cotton samples. This phenomenon may be surprising, as cotton samples loaded with TiO<sub>2</sub> efficiently photodegrade both RhB and MB dyes. However, it should be emphasised that the photodegradation of the RhB and

MB dyes was carried out in the dye solutions, the colour fastness of the curcumin dye was investigated on dry cotton samples. It is evident that for the photocatalytic activity of  $\text{TiO}_2$ , a sufficient amount of water must be absorbed at the surface of the  $\text{TiO}_2$

particles to generate reactive hydroxyl radicals. At the same time,  $\text{TiO}_2$  acted as a UV absorber on the textile surface, which significantly reduced the dose of UV rays reaching the curcumin dye and causing its photodegradation.

Table 4: Colour fastness to light of the chemically modified cotton samples

Sample	Illumination time (h)	$L^*$	$a^*$	$b^*$	$\Delta E^*_{ab}$
C5	0	89.87	-5.73	76.24	74.90
	72	93.54	-0.25	1.63	
C5-T	0	90.16	-5.97	50.75	51.14
	72	94.03	-0.33	0.07	
C5+T	0	73.94	10.11	44.95	47.68
	72	93.24	-0.34	2.62	

## 4 Conclusion

A novel green process for the chemical modification of cotton fabric was developed using the combination of curcumin dye and  $\text{TiO}_2$  to adjust the simultaneous photocatalytic activity and UV protection properties. During development, the influence of concentration of the turmeric extract and the two application processes on the functional properties of the chemically modified cotton fabric was thoroughly investigated. It was found that the optimum functional properties of the cotton fabric were achieved when the lowest concentration (5 g/L) of turmeric extract was applied and that the greener process including the simultaneous dyeing of cotton samples with turmeric extract and in-situ synthesis of  $\text{TiO}_2$  was more beneficial than the classical process in which the cotton sample was first dyed with turmeric extract and then in-situ synthesis of  $\text{TiO}_2$  was performed on the dyed sample.

It was found that the presence of the curcumin dye did not cause any visible morphological changes in the cellulose fibres, while the in-situ synthesis of  $\text{TiO}_2$  particles resulted in an increase in the roughness of the cellulose fibres with a clearly visible thin  $\text{TiO}_2$  coating containing many small and larger  $\text{TiO}_2$  agglomerates. The application of both the curcumin dye and  $\text{TiO}_2$  did not lead to significant changes in

the chemical structure of the cellulose fibres. Hydrothermal in-situ synthesis of  $\text{TiO}_2$  was promoted in turmeric extract compared to water, resulting in a higher total  $\text{TiO}_2$  content in the sample compared to that chemically modified in the absence of turmeric extract. As the hydrothermal in-situ synthesis of  $\text{TiO}_2$  was carried out at 120 °C, an amorphous structure of  $\text{TiO}_2$  was obtained in the chemically modified cotton sample.

The combination of the curcumin dye and  $\text{TiO}_2$  in the chemically modified cotton sample drastically improved the UV protection properties, resulting in a UPF value of 53.24, which corresponds to excellent protection. While  $\text{TiO}_2$  alone provided excellent UV protection in the UVB region, the curcumin dye significantly reduced the transmission of the sample in the UVA region, representing a synergistic effect between the two players. The presence of curcumin did not hinder the photocatalytic activity of  $\text{TiO}_2$  under visible light, but it also did not act as a sensitizer for  $\text{TiO}_2$ . This indicates that the chemical modification process developed did not create a curcumin- $\text{TiO}_2$  heterojunction with visible-light-driven photocatalysis. The inhibition of the photodegradation of the curcumin dye in the presence of  $\text{TiO}_2$  also confirmed the compatibility of the two players in the chemically modified cotton samples.

### Acknowledgments

This research was carried out within the framework of the courses on Advanced Finishing Processes and Chemical Functionalisation of Textiles in the Master Study Programme for Textile and Clothing Planning. The research was co-funded by the Slovenian Research and Innovation Agency (Programme P2-0213 Textiles and Ecology, Infrastructural Centre RIC UL-NTF).

### References

1. RIVERO, P.J., URRUTIA, A., GOICOECHEA, J., ARREGUI, F.J. Nanomaterials for functional textiles and fibers. *Nanoscale Research Letters*, 2015, **10**, 1–22, doi: 10.1186/s11671-015-1195-6.
2. PRINIOTAKIS, G., MARROT, L., STACHEWICZ, U., KRSTIC-FURUNDZIC, A., VENTURINI, E., JONAITIENE, V. Smart textile for building and living. *Autex Research Journal*, 2022, **22**(4), 493–496, doi: 10.2478/aut-2021-0041.
3. SHAH, M.A., PIRZADA, B.M., PRICE, G., SHIBIRU, A.L., QURASHI, A. Applications of nanotechnology in smart textile industry: a critical review. *Journal of Advanced Research*, 2022, **38**, 55–75, doi: 10.1016/j.jare.2022.01.008.
4. POPESCU, M., UNGUREANU, C. Green nanomaterials for smart textiles dedicated to environmental and biomedical applications. *Materials (Basel)*, 2023, **16**(11), 1–27, doi: 10.3390/ma16114075.
5. RADETIĆ, M. Functionalization of textile materials with TiO<sub>2</sub> nanoparticles. *Journal of Photochemistry and Photobiology C: Photochemistry Reviews*, 2013, **16**, 62–76, doi: 10.1016/j.jphotochemrev.2013.04.002.
6. RASHID, M.M., SIMONČIČ, B., TOMŠIČ, B. Recent advances in TiO<sub>2</sub>-functionalized textile surfaces. *Surfaces and Interfaces*, 2021, **22**, 1–33, doi: 10.1016/j.surfin.2020.100890.
7. ETACHERI, V., DI VALENTIN, C., SCHNEIDER, J., BAHNEMANN, D., PILLAI, S.C. Visible-light activation of TiO<sub>2</sub> photocatalysts: advances in theory and experiments. *Journal of Photochemistry and Photobiology C: Photochemistry Reviews*, 2015, **25**, 1–29, doi: 10.1016/j.jphotochemrev.2015.08.003.
8. NAM, Y., LIM, J.H., KO, K.C., LEE, J.Y. Photocatalytic activity of TiO<sub>2</sub> nanoparticles: a theoretical aspect. *Journal of Materials Chemistry A*, 2019, **7**, 13833–13859, doi: 10.1039/c9ta03385h.
9. EID, B.M., IBRAHIM, N.A. Recent developments in sustainable finishing of cellulosic textiles employing biotechnology. *Journal of Cleaner Production*, 2021, **284**, 1–22, doi: 10.1016/j.jclepro.2020.124701.
10. WANG, X., JIANG, J., GAO, W. Reviewing textile wastewater produced by industries: characteristics, environmental impacts, and treatment strategies. *Water Science & Technology*, 2022, **85**(7), 2076–2096, doi: 10.2166/wst.2022.088.
11. RAJ, A., CHOWDHURY, A., ALI, S.W. Green chemistry: its opportunities and challenges in colouration and chemical finishing of textiles. *Sustainable Chemistry and Pharmacy*, 2022, **27**, 1–17, doi: 10.1016/j.scp.2022.100689.
12. HUSTON, M., DEBELLA, M., DIBELLA, M., GUPTA, A. Green synthesis of nanomaterials. *Nanomaterials*, 2021, **11**(8), 1–29, doi: 10.3390/nano11082130.
13. SAMUEL, M.S., RAVIKUMAR, M., JOHN, A., SELVARAJAN, E., PATEL, H., CHANDER, P.S., SOUNDARYA, J., VUPPALA, S., BALAJI, R., CHANDRASEKAR, N. A review on green synthesis of nanoparticles and their diverse biomedical and environmental applications. *Catalysts*, 2022, **12**(5), 1–24, doi: 10.3390/catal12050459.
14. GUPTA, D., BOORA, A., THAKUR, A., GUPTA, T.K. Green and sustainable synthesis of nanomaterials: recent advancements and limitations. *Environmental Research*, 2023, **231**(3), 1–18, doi: 10.1016/j.envres.2023.116316.

15. NABI, G., QURAT-UL-AAIN; KHALID, N.R., TAHIR, M.B., RAFIQUE, M., RIZWAN, M., HUSSAIN, S., IQBAL, T., MAJID, A. A review on novel eco-friendly green approach to synthesis TiO<sub>2</sub> nanoparticles using different extracts. *Journal of Inorganic and Organometallic Polymers and Materials*, 2018, **28**, 1552–1564, doi: 10.1007/s10904-018-0812-0.
16. ILYAS, M., WARIS, A., KHAN, A.U., ZAMEL, D., YAR, L., BASET, A., MUHAYMIN, A., KHAN, S., ALI, A., AHMAD, A. Biological synthesis of titanium dioxide nanoparticles from plants and microorganisms and their potential biomedical applications. *Inorganic Chemistry Communications*, 2021, **133**, 1–9, doi: 10.1016/j.inoche.2021.108968.
17. IRSHAD, M.A., NAWAZ, R., UR REHMAN, M.Z., ADREES, M., RIZWAN, M., ALI, S., AHMAD, S., TASLEEM, S. Synthesis, characterization and advanced sustainable applications of titanium dioxide nanoparticles: a review. *Ecotoxicology and Environmental Safety*, 2021, **212**, 1–14, doi: 10.1016/j.ecoenv.2021.111978.
18. GONÇALVES, R.A., TOLEDO, R.P., JOSHI, N., BERENGUE, O.M. Green synthesis and applications of ZnO and TiO<sub>2</sub> nanostructures. *Molecules*, 2021, **26**(8), 1–39, doi: 10.3390/molecules26082236.
19. SAGADEVAN, S., IMTEYAZ, S., MURUGAN, B., LETT, J.A., SRIDEWI, N., WELDEGEBRIEAL, G.K., FATIMAH, I., OH, W.-C. A comprehensive review on green synthesis of titanium dioxide nanoparticles and their diverse biomedical applications. *Green Processing and Synthesis*, 2022, **11**, 44–63, doi: 10.1515/gps-2022-0005.
20. SHIVA SAMHITHA, S., RAGHAVENDRA, G., QUEZADA, C., HIMA BINDU, P. Green synthesized TiO<sub>2</sub> nanoparticles for anticancer applications: mini review. *Materials Today: Proceedings*, 2022, **54**(3), 765–770, doi: 10.1016/j.matpr.2021.11.073.
21. SINGH JASSAL, P., KAUR, D., PRASAD, R., SINGH, J. Green synthesis of titanium dioxide nanoparticles: development and applications. *Journal of Agriculture and Food Research*, 2022, **10**, 1–14, doi: 10.1016/j.jafr.2022.100361.
22. VERMA, V., AL-DOSSARI, M., SINGH, J., RAWAT, M., KORDY, M.G.M., SHABAN, M. A review on green synthesis of TiO<sub>2</sub> NPs: synthesis and applications in photocatalysis and antimicrobial. *Polymers (Basel)*, 2022, **14**(7), 1–19, doi: 10.3390/polym14071444.
23. DOSOKY, N.S., SETZER, W.N. Chemical composition and biological activities of essential oils of curcuma species. *Nutrients*, 2018, **10**(9), 1–42, doi: 10.3390/nu10091196.
24. STATI, G., SANCILIO, S., BASILE, M., ANGELELLI, A., DI PIETRO, R. *Curcuma longa* aqueous extract: a potential solution for the prevention of corneal scarring as a result of pterygium surgical excision (review). *International Journal of Molecular Medicine*, 2020, **46**(6), 1951–1957, doi: 10.3892/ijmm.2020.4738.
25. FULORIA, S., MEHTA, J., CHANDEL, A., SEKAR, M., RANI, N.N.I.M., BEGUM, M.Y., SUBRAMANIYAN, V., CHIDAMBARAM, K., THANGAVELU, L., NORDIN, R., WU, Y.S., SATHASIVAM, K.V., LUM, P.T., MEENAKSHI, D.U., KUMARASAMY, V., AZAD, A.K., FULORIA, N.K. A comprehensive review on the therapeutic potential of *Curcuma longa* Linn. in relation to its major active constituent curcumin. *Frontiers in Pharmacology*, 2022, **13**, 1–27, doi: 10.3389/fphar.2022.820806.
26. SELVAM, R.M., ATHINARAYANAN, G., NANTHINI, A.U.R., SINGH, A.J.A.R., KALIRAJAN, K., SELVAKUMAR, P.M. Extraction of natural dyes from *Curcuma longa*, *Trigonella foenum graecum* and *Nerium oleander*, plants and their application in antimicrobial fabric. *Industrial Crops and Products*, 2015, **70**, 84–90, doi: 10.1016/j.indcrop.2015.03.008.
27. JOSE, S., GURUMALLESH PRABU, H., AMMAYAPPAN, L. Eco-friendly dyeing of silk and cotton textiles using combination of three natural colorants. *Journal of Natural Fibers*, 2017, **14**(1), 40–49, doi: 10.1080/15440478.2015.1137530.

28. PERKIČ, N., GORJANC, M. Vpliv poobdelav na obarvljivost surovega in beljenega bombaža s kurkuminom in doseganje motivov s tehniko antotipije. *Tekstilec*, 2017, **60**(1), 4–13, doi: 10.14502/Tekstilec2017.60.4-13.
29. GORJANC, M., MOZETIČ, M., VESEL, A., ZAPLOTNIK, R. Natural dyeing and UV protection of plasma treated cotton. *The European Physical Journal D*, 2018, **72**, 1–6, doi: 10.1140/epjd/e2017-80680-9.
30. KABIR, S.M.M., HASAN, M.M., UDDIN, M.Z. Novel approach to dye polyethylene terephthalate (PET) fabric in supercritical carbon dioxide with natural curcuminoid dyes. *Fibres & Textiles in Eastern Europe*, 2019, **27**, 65–70, doi: 10.5604/01.3001.0013.0744.
31. TOPRAK-CAVDUR, T., UYSAL, S., GIBERT-PAYA, J. Dyeing recycled cotton fibers using *Curcuma longa* and *Pterocarpus santalinus* natural dyes and bio-mordant chitosan. *Journal of Natural Fibers*, 2022, **19**(16), 13736–13752, doi: 10.1080/15440478.2022.2105469.
32. BUDDEE, S., WONGNAWA, S., SRIPRANG, P., SRIWONG, C. Curcumin-sensitized TiO<sub>2</sub> for enhanced photodegradation of dyes under visible light. *Journal of Nanoparticle Research*, 2014, **16**, 1–21, doi: 10.1007/s11051-014-2336-z.
33. ABDUL JALILL, R.D., NUAMAN, R.S., ABD, A.N. Biological synthesis of titanium dioxide nanoparticles by *Curcuma longa* plant extract and study its biological properties. *World Scientific News*, 2016, **49**(2), 204–222.
34. LIM, J., BOKARE, A.D., CHOI, W. Visible light sensitization of TiO<sub>2</sub> nanoparticles by a dietary pigment, curcumin, for environmental photochemical transformations. *RSC Advances*, 2017, **7**, 32488–32495, doi: 10.1039/c7ra05276f.
35. RUHANE, T.A., ISLAM, M.T., RAHAMAN, M.S., BHUIYAN, M.M.H., ISLAM, J.M.M., NEWAZ, M.K., KHAN, K.A., KHAN, M.A. Photo current enhancement of natural dye sensitized solar cell by optimizing dye extraction and its loading period. *Optik*, 2017, **149**, 174–183, doi: 10.1016/j.ijleo.2017.09.024.
36. DIL, M.A., HAGHIGHATZADEH, A., MAZINANI, B. Photosensitization effect on visible-light-induced photocatalytic performance of TiO<sub>2</sub>/chlorophyll and flavonoid nanostructures: kinetic and isotherm studies. *Bulletin of Materials Science*, 2019, **42**, 1–16, doi: 10.1007/s12034-019-1927-9.
37. KABIR, F., BHUIYAN, M.M.H., HOSSAIN, M.R., BASHAR, H., RAHAMAN, M.S., MANIR, M.S., ULLAH, S.M., UDDIN, S.S., MOLLAH, M.Z.I., KHAN, R.A., et al. Improvement of efficiency of dye sensitized solar cells by optimizing the combination ratio of natural red and yellow dyes. *Optik*, 2019, **179**, 252–258, doi: 10.1016/j.ijleo.2018.10.150.
38. ANOUA, R., LIFI, H., TOUHTOUH, S., EL JOUAD, M., HAJJAJI, A., BAKASSE, M., PŁOCIENNIK, P., ZAWADZKA, A. Optical and morphological properties of *Curcuma longa* dye for dye-sensitized solar cells. *Environmental Science and Pollution Research*, 2021, **28**, 57860–57871, doi: 10.1007/s11356-021-14551-9.
39. VENKATAS, J., DANIELS, A., SINGH, M. The Potential of curcumin-capped nanoparticle synthesis in cancer therapy: a green synthesis approach. *Nanomaterials*, 2022, **12**(18), 1–23, doi: 10.3390/nano12183201.
40. BERGER-SCHUNN, A. *Practical color measurement*. New York : John Wiley Sons, 1994, p. 39.
41. SIST EN 13758-1:2002. Textiles - Solar UV protective properties - Part 1: Method of test for apparel fabrics. 12 p.
42. SIRIRERKRATANA, K., KEMACHEEVAKUL, P., CHUANGCHOTE, S. Color removal from wastewater by photocatalytic process using titanium dioxide-coated glass, ceramic tile, and stainless steel sheets. *Journal of Cleaner Production*, 2019, **215**, 123–130, doi: 10.1016/j.jclepro.2019.01.037.
43. ZHAO, H., KWAK, J.H., CONRAD ZHANG, Z., BROWN, H.M., AREY, B.W., HOLLADAY, J.E. Studying cellulose fiber structure by SEM, XRD, NMR and acid hydrolysis. *Carbohydrate*

- Polymers*, 2007, **68**(2), 235–241, doi: 10.1016/j.carbpol.2006.12.013.
44. ARBUJ, S.S., HAWALDAR, R.R., MULIK, U.P., WANI, B.N., AMALNERKAR, D.P., WAGH-MODE, S.B. Preparation, characterization and photocatalytic activity of TiO<sub>2</sub> towards methylene blue degradation. *Materials Science and Engineering: B*, 2010, **168**(1–3), 90–94, doi: 10.1016/j.mseb.2009.11.010.
45. KIM, M.G., KANG, J.M., LEE, J.E., KIM, K.S., KIM, K.H., CHO, M., LEE, S.G. Effects of calcination temperature on the phase composition, photocatalytic degradation, and virucidal activities of TiO<sub>2</sub> nanoparticles. *ACS Omega*, 2021, **6**(16), 10668–10678, doi: 10.1021/acsomega.1c00043.
46. RASHID, M.M., ZORC, M., SIMONČIČ, B., JERMAN, I., TOMŠIČ, B. In-situ functionalization of cotton fabric by TiO<sub>2</sub>: the influence of application routes. *Catalysts*, 2022, **12**(11), 1–17, doi: 10.3390/catal12111330.
47. SOCRATES, G. *Infrared and raman characteristic group frequencies: tables and charts*. 3rd edition. New York : John Wiley & Sons, 2004.
48. ROHAETI, E., RAFI, M., SYAFITRI, U.D., HERYANTO, R. Fourier transform infrared spectroscopy combined with chemometrics for discrimination of *Curcuma longa*, *Curcuma xanthorrhiza* and *Zingiber cassumunar*. *Spectrochimica Acta, Part A: Molecular and Biomolecular Spectroscopy*, 2015, **137**, 1244–1249, doi: 10.1016/j.saa.2014.08.139.
49. BÖTTCHER, H., MAHLTIG, B., SARSOUR, J., STEGMAIER, T. Qualitative investigations of the photocatalytic dye destruction by TiO<sub>2</sub>-coated polyester fabrics. *Journal of Sol-Gel Science and Technology*, 2010, **55**, 177–185, doi: 10.1007/s10971-010-2230-9.
50. ZHOU, Y., TANG, R.C. Influence of fixing treatment on the color fastness and bioactivities of silk fabric dyed with curcumin. *The Journal of The Textile Institute*, 2017, **108**(6), 1050–1056, doi: 10.1080/00405000.2016.1219447.